PAPER

NJC
www.rsc.org/njc

Silver organosol: synthesis, characterisation and localised surface plasmon resonance study†

Sudip Nath, Sujit Kumar Ghosh, Snigdhamayee Praharaj, Sudipa Panigrahi, Soumen Basu and Tarasankar Pal*

Department of Chemistry, Indian Institute of Technology, Kharagpur 721 302, India. E-mail: tpal@chem.iitkgp.ernet.in

Received (in Montpellier, France) 20th June 2005, Accepted 24th August 2005
First published as an Advance Article on the web 20th October 2005

In this article a simple and reproducible technique for the synthesis of a silver organosol is reported from a specific silver precursor, solid silver acetate. Molten hexadecylamine acts as a solvent for silver acetate and imparts stability to the evolved nanoparticles. The amine-capped organosol shows unique stability as neither agglomeration nor oxidation takes place over one year. The synthesised silver particles have been characterised by UV-visible, TEM, XRD, XPS, FTIR and thermogravimetric studies. The hexadecylamine-stabilised silver organosol was employed to examine the altered optical properties in different solvent systems and with different ligands by accounting for the changes in the localised surface plasmon resonance (LSPR) spectrum. It was observed that the position of the surface plasmon band of silver nanoparticles is greatly affected by the solvents and ligands under consideration. The quantitative alteration of the LSPR spectrum involving encapsulated nanoparticles in a dielectric ligand shell has been rationalised from Mie theory. It has also been shown that cationic and anionic surfactants of different chain lengths induce changes in the optical properties of silver nanoparticles whereas, zwitterionic amino acid molecules reflect insignificant changes in the LSPR spectrum. The λ_{max} of the LSPR gradually shifts to red with the increase in chain length of both the cationic and anionic surfactants, indicating specific binding of the surfactant molecules around silver nanoparticles. Finally the affinity of the synthesised silver nanoparticles for amine molecules has been accounted for by taking the HSAB principle into consideration.

Introduction

A growing research interest has been directed towards the synthesis, characterisation and study of metal colloids in organic solvents.[1–6] Metal organosols are convenient objects for the investigation of the physicochemical properties of metallic nanoparticles,[7,8] and for their unusual optical and catalytic behaviour. The high surface energy of the nanoparticles[9,10] and consequently their tendency for agglomeration, hinders their preparation in high concentration in an aqueous system. The use of organic solvents, instead of aqueous ones, might be a promising solution to this problem where the particles suffer fewer encounters between themselves due to the presence of giant hydrophobic stabilising ligands. Moreover nanoparticles in organic media are becoming an interesting subject with a view to studying several optical phenomena.[11]

The optical properties of noble metal nanoclusters have fascinated scientists in recent years because of their applications as functional materials in optical devices,[12] optical energy transport,[13,14] near field scanning optical microscopy,[15–17] plasmonic devices,[18–20] and biological sensors.[21–26] The intense scattering and absorption of light from metals in their nano regime has motivated researchers in studying their optoelectronic behaviour to a great extent. Noble metal nanoparticles like silver exhibit a strong absorption band in the visible region, which is indeed a small particle effect, since it is absent in the individual atom as well as in the bulk.[27–35] This absorption band results when the incident photon frequency is resonant with the collective oscillation of the conduction electrons and is known as localised surface plasmon resonance (LSPR). In 1908, Mie[36] first described this phenomenon theoretically by solving Maxwell's equations for a radiation field interacting with a spherical metal particle under appropriate boundary conditions. The only material-related functions and constants in Mie theory are the complex dielectric function of the metal and the dielectric constant of the surrounding medium. In particular, the peak extinction wavelength, λ_{max}, of the LSPR spectrum is unexpectedly sensitive to nanoparticle size, shape and local dielectric environment. Such sensitivity of the LSPR spectrum has motivated researchers to investigate the optical properties of metal clusters to a great extent.[37]

Among all the metals silver is an important one[38–42] to study at its nanoscale due to the frequency-dependent behaviour of its complex dielectric constant and its application in surface enhanced Raman scattering.[43–45] Preparation of silver nanoparticles in an organic solvent is at the forefront of many research activities because of their unusual optical properties in varied solvents.[46,47] Ag nanoparticle-based LSPR nanosensor yields ultra-sensitive biodetection techniques with extremely simple, small and low-cost instrumentation. Thus, it is desirable to design synthetic methods that lead to stabilisation of silver nanoparticles in various solvents. Furthermore, in order to systematically study the LSPR response, it is desired to synthesise monodispersed metal nanoparticles with a narrow size distribution. An inhomogeneous size distribution complicates the correlation between theory and experiment.[48,49] A few ingenious methodologies have been devised pertaining to the synthesis of silver organosols,[50] most of which were based on the phase-transfer procedure.[51,52] Such a synthetic route leads to an organosol system contaminated with phase-transfer and

† Electronic supplementary information (ESI) available: TEM image of silver nanoparticles dispersed in THF after one year. See http://dx.doi.org/10.1039/b508730a

DOI: 10.1039/b508730a

reducing agents, which is a major drawback for spectroscopic applications. Thus, controlled synthesis of silver organosols and the systematic study of their optical properties in a sequence of solvents are still under investigation and are the basis of several fundamental research projects.

In the present article we report a simple procedure for the synthesis of a stable silver organosol as well as solid silver nanoparticles (on the gram scale) capped with hexadecylamine (HDA). As far as the stability is concerned, this is a unique route for the synthesis of a silver organosol in which the particles remain stable over one year. Particles have been characterised through UV-visible, transmission electron microscopy (TEM), X-ray photoelectron spectroscopy (XPS), X-ray diffraction (XRD), Fourier-transform infrared spectroscopy (FTIR) and thermogravimetric studies. The organosols synthesised in this manner were made free from excess capping as well as reducing agent and exploited to study the optical properties when exposed to various solvents and ligands by measuring the changes in the LSPR of the metal particles. Again, the HDA-capped silver organosol was subjected to interactions with cationic and anionic surfactants of different chain length to study the LSPR. Finally the affinity of the synthesised silver particles for amine molecules is accounted for by taking the HSAB principle into consideration.

Experimental

Reagents

All the reagents used were of AR grade. Doubly distilled water was used throughout the experiment. Silver acetate ($AgOOCCH_3$) was purchased from Aldrich. Hexadecylamine was received from Merck. Acetaldehyde was purchased from S. D. Fine Chemicals, India and was distilled before use. All the solvents used were purchased from Merck and dried before use. Cetyltrimethylammonium chloride (C_{16}TAC) and other cationic surfactants of different (C_{10}, C_{12}, C_{14} and C_{18}) chain length of the homologous series were obtained from Aldrich and were used without further purification. Anionic surfactants, decyl sodium sulfate (DSS), sodium dodecyl sulfate (SDS), and sodium dodecyl benzene sulfonate (SDBS) were purchased from Sigma and were used as received.

Instruments

Absorption spectra were recorded on a Spectrascan UV 2600 spectrophotometer (Chemito, India) taking the solutions in a 1 cm quartz cuvette. Normalised spectra were taken, always subtracting the solvent background. TEM measurements were made on a Hitachi H-9000 NAR instrument at a magnification of 100 k. The sample was prepared by placing a drop of the solution on a carbon-coated copper grid. The sample was diluted in THF before spotting. The solid silver particles were analysed by XRD, XPS, FTIR and thermogravimetric studies. XRD was done using a PW1710 diffractometer (Philips, Holland) instrument. The XRD data were analysed using JCPDS software.[72] XPS were done in ESCALAB-MK-II, UK. FTIR was done using a Nexus 870 Thermo-Nicolet instrument coupled with a Thermo-Nicolet continuum FTIR microscope. Thermal measurements were carried out with a thermogravimetric instrument, Perkin-Elmer, DSC7.

Procedure

20 g solid HDA (8.28×10^{-2} mole) was heated to melt ($\sim$50 °C) in an oil bath and solid silver precursor, in the form of silver acetate (2 g, 0.012 mole), was dissolved in it. Thus HDA acts as a solvent for silver acetate under molten conditions and proportions of 10 : 1 (w/w for HDA : silver acetate) are to be maintained for the complete dissolution of silver acetate in HDA. Then, the resulting mixture was stirred using a magnetic stirrer and treated with 5 ml acetaldehyde (distilled) to reduce Ag(I) to Ag(0). Afterwards, 200 ml methanol was added dropwise to the hot solution, to increase the polarity of the medium, and consequently solid nanoparticles selectively precipitated out in mass. Then the resulting precipitate was centrifuged and washed several times with methanol to remove the free capping agent, HDA. Finally, the as-synthesised nanoparticles were dried and stored as solid silver nanoparticles. The weight of the HDA-capped solid silver nanoparticles was found to be 1.5 g. The particles were redispersed in several polar and non-polar solvents *viz*. tetrahydrofuran (THF), toluene, acetonitrile, cyclohexane *etc*. to obtain the desired HDA-capped silver organosol in varied solvent systems.

LSPR study

The dependence of surface plasmon band position on the solvent refractive index was studied by dispersing the silver organosol in different solvents. In practice solid silver nanoparticles ($\sim$0.1 g) were dispersed in 10 ml THF and consequently the concentration of the resulting solution becomes $\sim$0.1 M. An aliquot of 20 μl of this highly concentrated silver suspension was then diluted to 2 ml with the desired solvents so that the final concentration of the sol becomes $\sim$1 mM and the THF content of the final suspension becomes $\sim$1%.

A measured amount of either surfactant or ligand solution (0.1 mM) in THF was introduced to the silver suspension ($\sim$1 mM) and the final volume was adjusted to 2 ml for measurements of changes in LSPR induced by the ligand.

Results and discussion

Transmission electron microscopy

Fig. 1(a) shows a TEM image of the HDA-capped silver nanoparticles. As shown from the TEM image, the HDA-capped silver nanoparticles are spherical in shape with a particle size of 10 $\pm$ 2 nm having a hexagonal closed pack symmetry. It is also found that each particle is well separated from the neighbouring nanoparticles, indicating that the silver nanoparticles are well surface passivated by HDA molecules. The histogram [Fig. 1(b)] of the particles shows that the as-prepared materials have a tight size distribution. The histogram was obtained by analysing 100 particles from different portions of the grid.

It is obvious that the silver nanoparticles of larger sizes were believed to grow at the expense of smaller ones *via* an Ostwald ripening process, where small nanoparticles dissolved and grew into larger crystals.[53] The crystal growth and dissolution of nanoclusters occur simultaneously. Therefore the formation of uniform and well-shaped particles can be accounted for as a consequence of a balance between stabilisation and crystal growth in the solvent. Due to the large surface-to-volume ratio of the nanosized particles the dissolution is much easier and thus the growth rate becomes comparatively slower because small particles often grow much more slowly than macrocrystals.[54] Consequently, a uniform size distribution is obtained at the end.

The stability of the nanoparticles towards agglomeration was authenticated from their unaltered microscopic image over a year. The particles are extremely stable towards agglomeration and retain same particle morphology in varied organic solvents as was confirmed from TEM measurements (see ESI†).

In contrast to water, the production of stable metallic colloids in organic media is quite a different matter. In this case electrostatic stabilisation is not effective due to the relatively low polarity of the organic medium. Therefore steric stabilisation is the key factor for the stability of the nanoparticles. In this case the amine functional group anchors to the silver surface and the long hexadecyl chain offers a huge

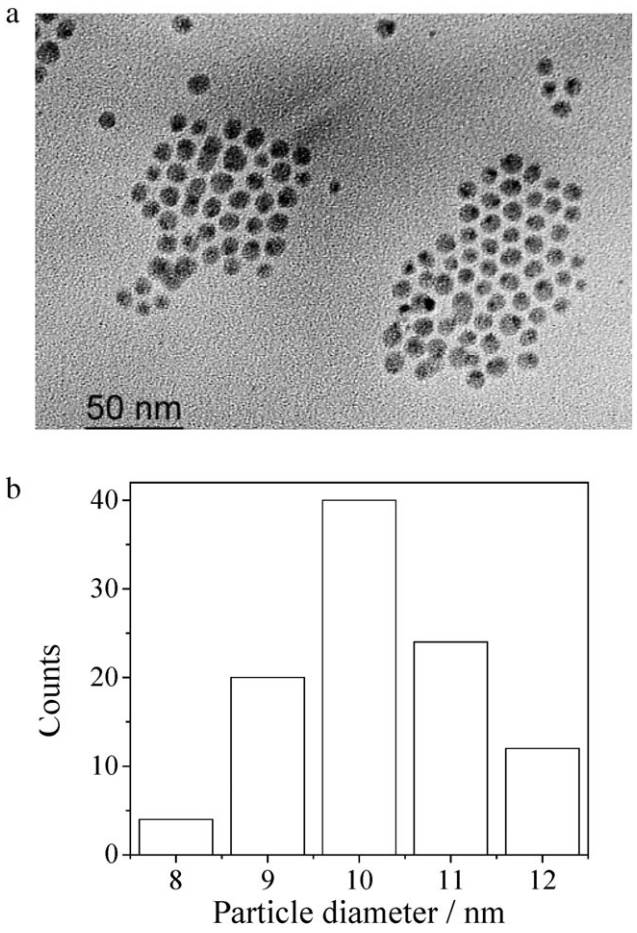

Fig. 1 (a) TEM image of HDA-capped silver organosol. (b) Corresponding diameter histogram of silver nanoparticles.

hydrophobic environment and imparts stabilisation to the colloids.

X-Ray photoelectron spectroscopy

The oxidation state of Ag in the HDA-capped Ag organosol was determined by X-ray photoelectron spectroscopy (Fig. 2). In this case solid nanoparticles were employed for the purpose. The amine-capped silver nanoparticles typically show a spectral profile exhibiting two peaks at 367 and 373 eV due to $Ag3d_{\frac{5}{2}}$ and $Ag3d_{\frac{3}{2}}$ orbitals respectively, which indicates that the silver atoms present in the cluster must be present as Ag(0).

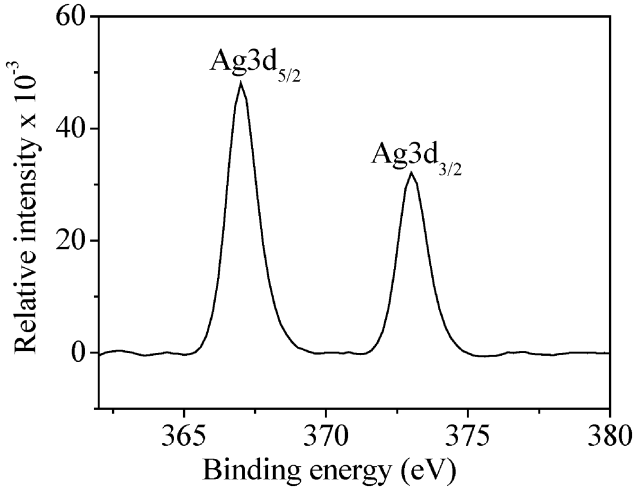

Fig. 2 X-Ray photoelectron spectroscopy of solid silver nanoparticles.

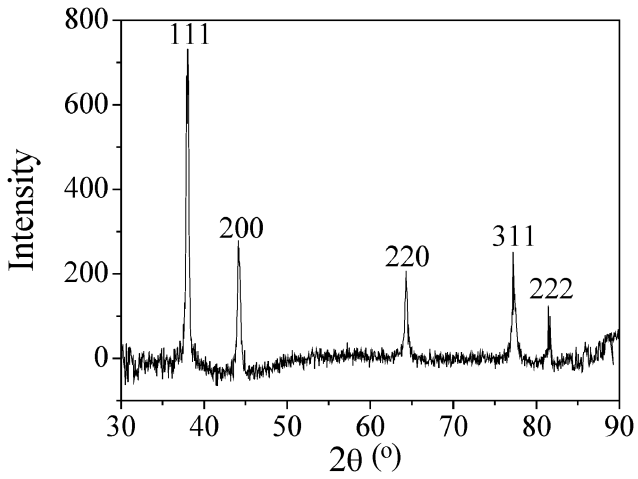

Fig. 3 X-Ray diffraction pattern of solid silver nanoparticles.

The unaltered spectral profile of the XPS image substantiates the stability of the nanoparticles against oxidation over the year.

X-Ray diffraction study

The X-ray diffraction pattern of the solid HDA-capped silver nanoparticles is shown in Fig. 3. The five diffraction peaks above 30°, corresponding to silver (111), (200), (220), (311), and (222), indicate the formation of silver nanocrystals with fcc structure.

FTIR analysis

The FTIR spectra of solid nanoparticles and of HDA show a similar pattern (Fig. 4), which indicates that HDA is indeed a part of the composite. The peak due to the N–H stretching mode of vibration which in free HDA appears at 3334 cm^{-1}, suffers a red shift of 100 cm^{-1}, supporting the notion that the amine head groups face the silver nanoparticle surfaces. The peaks due to the C–H stretching mode, which appear at 2919 (symmetric) and 2850 cm^{-1} (antisymmetric), are also red shifted and appear at 2926 and 2852 cm^{-1} respectively. This observation is well consistent with the previous results obtained for gold nanocrystals.[55]

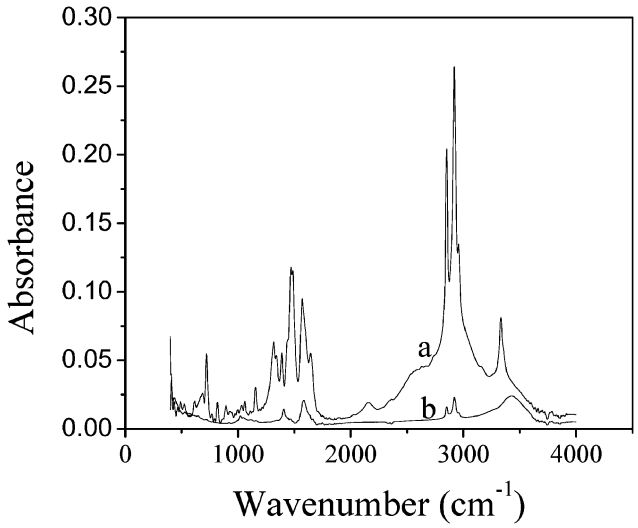

Fig. 4 FTIR spectra of (a) free HDA (b) HDA-capped silver nanoparticles.

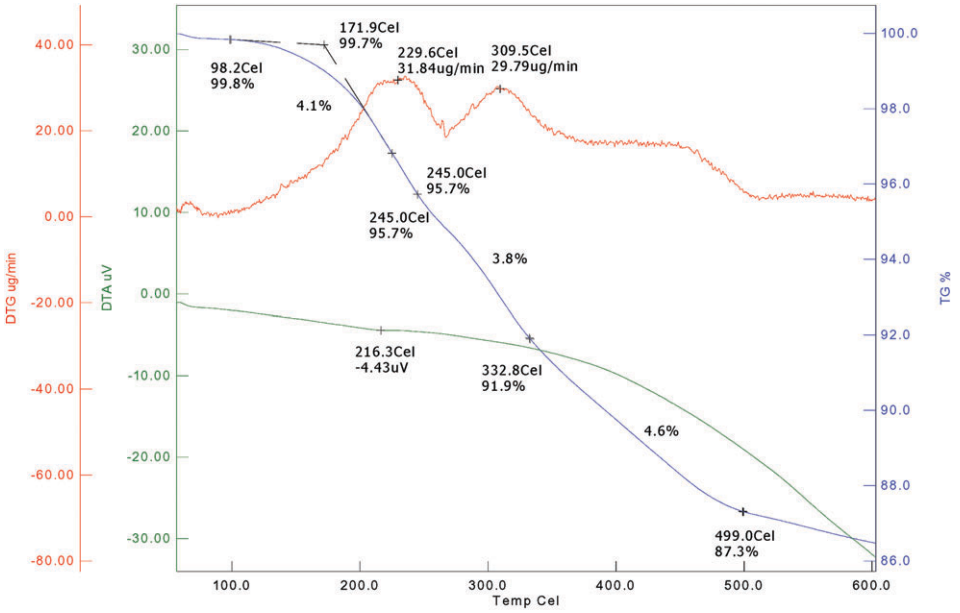

Fig. 5 DTA, TG and DTG curves of solid HDA-capped silver nanoparticles.

Thermogravimetric analysis

The attachment of HDA molecules to the surface of silver nanocrystals may conveniently be proved from thermogravimetric analysis (Fig. 5) of the solid particles. The amine-capped silver particles show three successive weight losses in the temperature region 100–500 °C. These weight losses can be attributed to the ready desorption of amine molecules from the surface of the silver nanocore. From the above observation it can be concluded that the HDA molecules are weakly bonded to the metal surface. The total weight loss is about 12.7%, and corresponds to the decomposition of organic material. This data is consistent with experimental observation: 2 g of silver acetate are expected to give 1.29 g of silver. As we obtained 1.5 g of HDA-capped silver nanoparticles, the metal only represents about 86% of the total weight. The remaining 14% compares nicely to the observed 12.7% weight loss and can be reasonably attributed to the capping HDA molecules.

UV-visible spectroscopy

HDA-capped silver organosol displays a strong absorption band at 410 nm [Fig. 6(a)] in THF, which can be assigned to the surface plasmon band of the silver clusters. The position and shape of the plasmon band is changed depending on the size, shape and dielectric constant of the medium. Such variation is obtained by dispersing the organosol in other organic solvents, and is the basis of several fundamental investigations encompassing the optical phenomenon of metallic colloids.[56,57]

The simplest theoretical approach available for modelling the optical properties of nanoparticles is the Mie theory estimation of the extinction of a metallic sphere in the long wavelength, electrostatic dipole limit which can be calculated from the following equation:[58]

$$E(\lambda) = \frac{24\pi N_A a^3 \varepsilon_m^{3/2}}{\lambda \ln(10)} \left[\frac{\varepsilon_i}{(\varepsilon_r + \chi\varepsilon_m)^2 + \varepsilon_i^2} \right] \qquad (1)$$

where, $E(\lambda)$ is the extinction (sum of absorption and scattering) energy, N_A is the areal density of nanoparticles, a is the radius of the metallic nanosphere, ε_m is the dielectric constant of the medium surrounding the metallic nanosphere (assumed to be a positive, real number and wavelength independent), λ is the wavelength of the absorbing medium, ε_r and ε_i are the real and imaginary part of the dielectric function of the metallic nanoparticles and χ is the aspect ratio of the particles. From the above equation it is clear that the LSPR spectrum of an isolated metallic nanoparticle depends on the particle radius

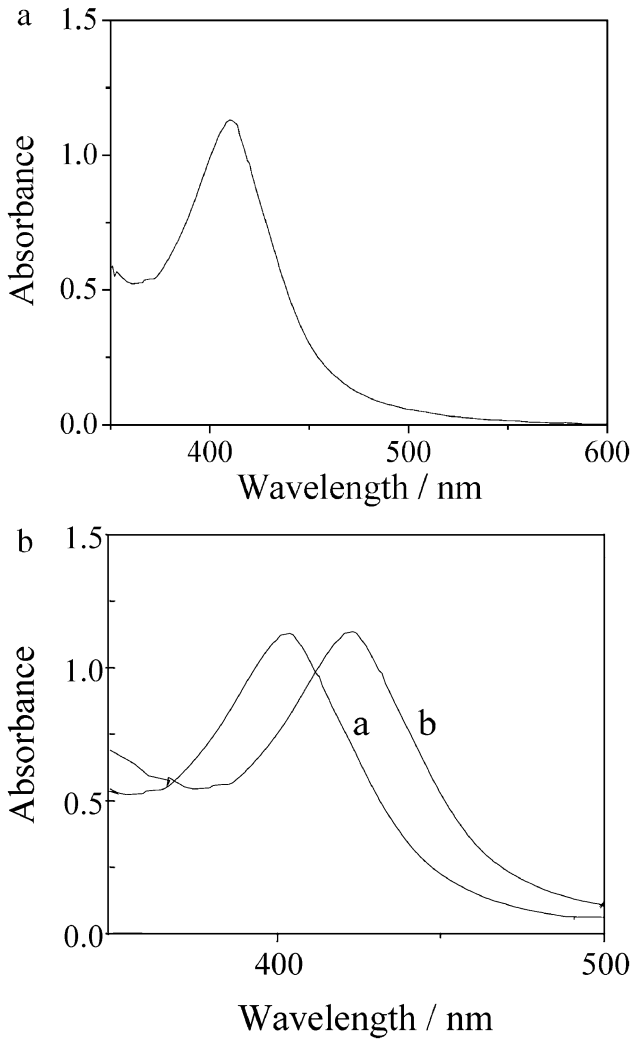

Fig. 6 (a) UV-visible spectrum of silver nanoparticles dispersed in THF. (b) Absorption spectra of silver organosol in: a cyclohexane; b 1,4-dioxane.

(a), nature of the particles (ε_r, ε_i) and dielectric constant of the local microenvironment (ε_m). It is obvious that the position of the extinction maximum of noble metal nanoparticles is highly dependent on the dielectric property of the surrounding environment and the resulting wavelength shift of the LSPR can be used to detect molecule-induced changes surrounding the nanoparticles.

LSPR of silver colloids

Effect of solvent. Fig. 6(b) shows the effect of medium dielectric constant on the absorption maxima of silver nanoparticles in cyclohexane (n 1.4262) and 1,4-dioxane (n 1.4224). A red shift of ~20 nm in the LSPR was observed when the solvent was substituted with 1,4-dioxane in place of cyclohexane. A similar spectral shift of 10 nm in the case of gold nanoparticles stabilised by a comb polymer was observed in an earlier case[59] when the solvent refractive index was varied from 1.3750 (hexane) to 1.5010 (benzene). The variation of the peak position with solvent refractive index for a wide range of solvents is shown in Table 1. A close inspection of the results shows that the HDA-capped silver nanoparticles follow two different trends in two types of solvents. In non-polar solvents like cyclohexane, chloroform, carbon tetrachloride, toluene and o-xylene, the variation of λ_{max} of the LSPR with the solvent refractive index follows a linear trend. In this case the λ_{max} of the LSPR gradually shifts to red with increasing solvent refractive index. On the other hand plasmon absorption maxima of the silver organosols vary with solvent refractive index without obeying a general trend in the polar solvents *viz.* acetonitrile, tetrahydrofuran, 1,4-dioxane, dimethylformamide, dimethyl sulfoxide. The above observation can be attributed to the fact[60] that non-polar solvents do not possess any added functional group to bind with the silver nanoparticles. Therefore, a linear dependence of the LSPR with solvent refractive index is observed for this type of solvent. In contrast, the polar solvents possess active functional groups which can directly interact with the metal surface through charge transfer and they have different electron injection capabilities. The silver atoms at the surface of the cluster are coordinatively unsaturated and consequently they strip electrons from such solvent molecules.[61] According to Mie theory[36] the addition and removal of electrons from colloidal particles results in a shift in the LSPR of the plasmon band position.[62,63] In this case the amount of available electrons from different solvent molecules is different and that results in the variation in the LSPR of the silver particles in these solvents. The resulting charged particles are stabilised by the solvent molecules, and the repulsive force between the charged particles prevents their aggregation.[64–66]

The linear variation of the maxima of LSPR with the refractive index of the non-polar solvents can be treated within the framework of the Drude model. According to the Drude model, the surface plasmon peak position, λ, is related to the refractive index of the surrounding medium (n) by the relation[32]

$$\lambda^2 = \lambda_p{}^2(\varepsilon^\alpha + 2\varepsilon_m) \quad (2)$$

where, λ_p is the bulk metal plasmon wavelength, ε^α is the high-frequency dielectric constant due to interband and core transitions, and ε_m ($= n^2$) is the optical dielectric function of the medium. From eqn (2), it is evident that a plot of λ^2 *vs.* $2\varepsilon_m$ gives the information about the bulk plasmon frequency of the metal. Fig. 7 shows a plot of the square of the observed plasmon band position (λ^2) of the LSPR of silver nanoparticles in a sequence of non-polar solvents, as a function of twice the medium dielectric function ($2\varepsilon_m$). The linear variation of the λ_{max} of the LSPR with the medium dielectric function is indicative of the fact that the solvent refractive index influences the surface plasmon maximum according to the Drude model. Therefore, it can be inferred that, although the HDA molecules surrounding the nanoparticle act as a barrier preventing solvent penetration to the surface, the electromagnetic fields of silver remain extended to sense refractive index changes in such solvents.

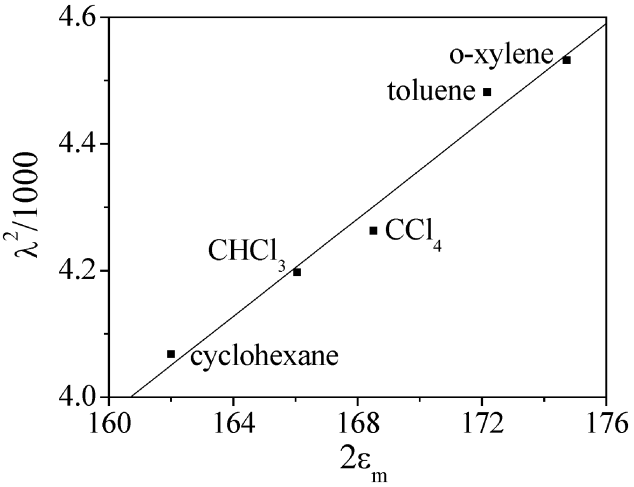

Fig. 7 A plot of the squares of the absorption maxima (λ^2) as a function of twice the medium dielectric constant ($2\varepsilon_m$) in different solvents.

Table 1 Absorption maxima of LSPR of HDA-capped silver nanoparticles in solvents of varying refractive indices

Solvent	Refractive index (n)	λ_{max} (nm)	Dielectric constant
Cyclohexane	1.4262	402.5	2.02
Chloroform	1.4486	407.5	4.81
Carbon tetrachloride	1.4600	410.5	2.24
Toluene	1.4969	414	2.38
o-Xylene	1.5054	423	2.56
Acetonitrile	1.3441	419	36.64
Tetrahydrofuran	1.4072	410	7.52
1,4-Dioxane	1.4224	423	2.22
Dimethylformamide	1.4282	414	38.25
Dimethyl sulfoxide	1.4790	422	47.24

Ligand binding effects. HDA-capped silver nanoparticles are stable in organic solvent systems as a consequence of the giant hydrophobic chain of the alkylamine stabiliser. The particles get encapsulated at the core of the stabilising agent and steric repulsion between the hydrocarbon chains imparts stability to the system. Encapsulation of the particle core with an appropriate shell material also offers a means of protection from the surrounding environment. These types of nanoparticles are commonly referred to as 'core-shell' particles, consisting of metal cores with a dielectric shell. Independent manipulation of the core and shell composition provides a way to engineer optical functionality. The incorporation of a shell material adds a new level of complexity to the electromagnetic modelling of the optical function due to the asymmetric environment. It is, therefore, important to understand how the interaction of the metal particles with the stabilising ligand influences the plasma resonance. Here, we have explored the response of the LSPR to the changes in refractive index induced by the ligand binding events to the HDA-capped silver nanoparticles. It has been found that the change in refractive index induced by analyte binding events could be detected from the change in the extinction wavelength response of the LSPR.

A series of cationic (C_{10}TAC, C_{12}TAC, C_{14}TAC, C_{16}TAC and C_{18}TAC) and anionic (DSS, SDS, and SDBS) surfactants of variable chain length has been selected to detect the changes in the LSPR of the silver nanoparticles. It was seen that surfactants with variable chain lengths induce different dielectric environments at the nanoparticle–surfactant interface and the sensitivity was reflected in the absorption spectra of the silver nanoparticles. Fig. 8(a) shows the effect of addition of cationic surfactants of two different chain lengths (C_{10} and C_{18}) on the LSPR of silver organosol. It was observed that with an increase of chain length of the cationic surfactant, a red shift in the LSPR of the extinction wavelength takes place. A similar effect on the LSPR was observed with the variation in chain length of anionic surfactants (DSS, SDS, and SDBS) as shown in Fig. 8(b). Although, introduction of zwitterionic amino acids does not result in any remarkable change in the LSPR under the same experimental conditions.

The effect of ligand chain length on the LSPR of silver colloids can be explained by considering the contribution of the dielectric environment of the organic shell. When a metallic nanoparticle is stabilised by a ligand shell whose refractive index is different from that of the ambient (*i.e.*, a silver nanocore), the field that acts on the particle is no longer homogeneous. The dense shell of binding ligands provides a dielectric coating on the particle surface, leading to a change in the dielectric constant of the medium and causing a red shift of the λ_{max} of the LSPR.[32,67,68] The silver nanocore are capped with the HDA molecules in the absence of any added surfactants or ligands. Now, introduction of surfactants of variable chain length induces adsorption of surfactant molecules on the surface of the silver particles through a 'place exchange reaction' with the HDA molecules.[69] In the present experiment, as both cationic and anionic surfactants cause a red shift in the absorption spectrum, it is reasonable to assume that alteration of the refractive index is an important factor in influencing the LSPR. In addition, in a system of metal particles where the combination of solvent and ligand shell is very similar in terms of refractive index, the particles may be treated as if they were in a homogeneous solvent. Murray *et al.*[70] thus modified eqn (2) by including the dielectric of the organic shell as

$$\lambda^2 = \lambda_p^2[(\varepsilon^\alpha + 2\varepsilon_m) - 2g(\varepsilon_m - \varepsilon_s)/3] \quad (3)$$

where, g is the volume fraction of the shell layer which increases with chain length of the organic capping agent and ε_s is the optical dielectric function of the shell layer. The medium is assumed to be non-absorbing so that ε_s is the dispersionless optical dielectric function of the shell and is related to the refractive index of the shell layer by the relation $\varepsilon_s = n^2$. The volume fraction of the shell layer, *i.e.* core-to-shell volume ratio (g) is defined as,

$$g = \frac{[(R_{core} + R_{shell})^3 - R_{core}^3]}{(R_{core} + R_{shell})^3} \quad (4)$$

where R_{core} and R_{shell} are the radii of the core and thickness of the shell respectively. The contribution of the g value becomes smaller as the particle size becomes larger. For very small particles ($\sim$2 nm), the sizes of core and organic shell become comparable and this in turn reduces the sensitivity of silver plasmon resonance to the changes in solvent refractive index. An increase of the solvent refractive index should cause a lowering of the surface plasmon band energy, but this value will be less pronounced as g increases.

Here, in this case the HDA-capped silver particles have diameter $\sim$10 nm and consequently the g value becomes small and the plasmon absorption maxima becomes sensitive to the change in solvent refractive index. The eqn (2) and (3) clearly show the contribution of the dielectric shell layer in the optical properties of silver nanoparticles. According to eqn (4), g increases with an increase of chain length of surfactant. As a result, the position of the plasmon band would be shifted towards a longer wavelength with an increase of chain length of the surfactant, which has been reflected in Fig. 8(a) and 8(b). Again, if the refractive index of monolayer, $n_s = \varepsilon_s^{\frac{1}{2}}$, increases (*e.g.* through the use of surfactants of increased chain length) the band wavelength should decrease. The absorption changes indicated the altered electronic state induced by the covalent linking of the metal nanocore. Since these ligands are intimately bound to the particle surface it is possible that they provide or withdraw electron density from the interface. The influence of such binding events on the bulk plasmon wavelength (λ_p) of the metal, owing to a change in free electron density, can be described as

$$\lambda_p = 2\pi c/\omega_p \quad (5)$$

where, c is the velocity of light in a vacuum and ω_p is the metal's bulk plasma frequency, given by

$$\omega_p = (Ne^2/m\varepsilon_0)^{\frac{1}{2}} \quad (6)$$

where, N is the free electron density and m is the electron mass.

The insignificant variation of the LSPR spectrum upon addition of amino acids of different chain lengths indicates non-specific interaction of the amino acid molecules with the HDA-capped silver particles.

The effect of ligand functionality has also been studied by introducing thiols of different chain length (C_{10}, C_{12}, C_{14} and C_{16}) to the amine-stabilised organosol system. In this case also,

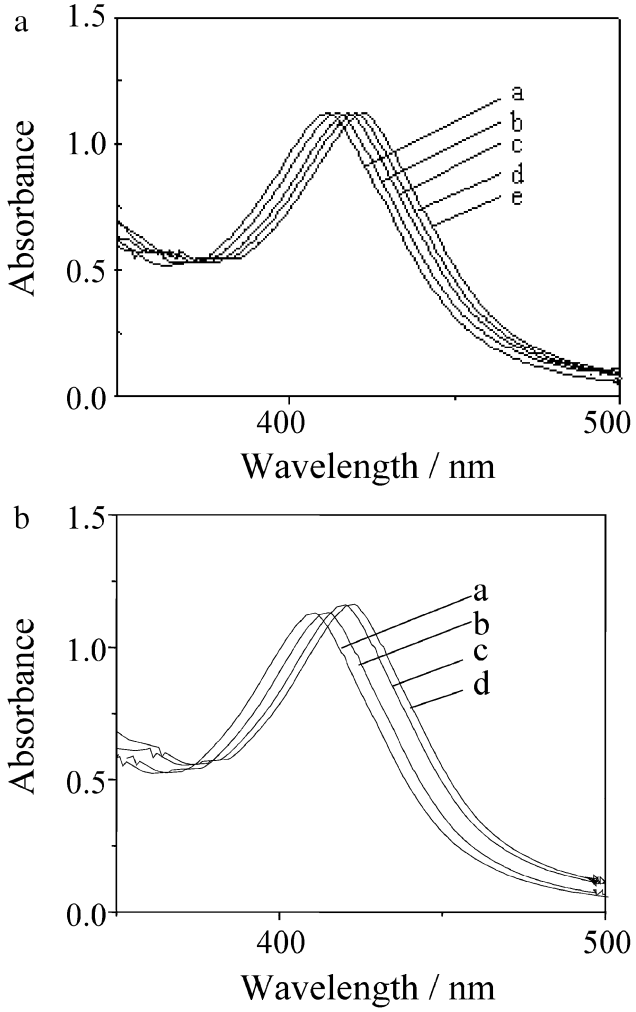

Fig. 8 (a) UV-visible spectra of silver organosol in the presence of: a C_{10}TAC; b C_{12}TAC; c C_{14}TAC; d C_{16}TAC; e C_{18}TAC. (b) Absorption spectra of silver nanoparticles in THF in the presence of: a no surfactant; b DSS; c SDS; d SDBS.

an insignificant change was observed. Such an effect can be attributed to the fact that silver has reasonable affinity for harder nitrogen as compared to softer sulfur.[71] Thus, thiol molecules of variable chain length are unable to induce significant interactions with silver nanocores capped with HDA molecules. Such an effect is a mere reflection of the HSAB principle, where stronger interaction of silver nanoparticles with amine molecules does not allow the thiol molecules to make significant changes in the LSPR of silver nanoparticles.

Conclusion

In conclusion, we have developed a route to synthesise HDA-capped silver nanoparticles which can be dispersed in varied organic solvents. Clearly, this is an exclusive report of the preparation of a stable silver organosol with unaltered morphology over a year. Moreover, this is a unique route to synthesise solid silver nanoparticles on the gram scale. The procedure is simple, reproducible and could be a general method for the direct synthesis of varied metal organosols in mass. The stable organosol system is devoid of any phase-transfer reagent, leading to the simple regeneration of the sol system in varied solvents without any contamination. Thus such a system may be a useful one for spectroscopic and optical applications. The characteristic optical absorption spectra of the silver organosol in different solvents provide information on the electronic structure of the metal particles. It has been found that the solvents influence LSPR in two different ways. The LSPR follows a linear variation with the refractive index of non-polar solvents, whereas in polar solvents the λ_{max} of the LSPR shifts without following any general trend. It has also been found that the introduction of a stabilising ligand shell also leads to a shift in the plasmon band position of the LSPR to a reasonable extent. The effect of increasing chain length of both cationic and anionic surfactants on the LSPR has also been accounted for by the contribution of the dielectric of the organic shell under consideration. Finally, the synthesised organosol might find a wide range of applications in chemical and biological sensors, molecular microelectronics and other optical applications with highly controllable optical properties. The solubility of the particles in a wide-range of polar and non-polar solvents might lead to an avenue for the preparation of heterogeneous catalysts in future.

Acknowledgements

The authors sincerely thank CSIR & UGC, New Delhi and IIT-Kharagpur for financial assistance.

References

1 Y. U. Seo, S. J. Lee and K. Kim, *Chem. Commun*., 2004, **6**, 664.
2 S. Praharaj, S. K. Ghosh, S. Nath, S. Kundu, S. Panigrahi, S. Basu and T. Pal, *J. Phys. Chem. B*, 2005, **109**, 13166.
3 S. Gao, J. Zhang, Y. Zhu and C. Che, *New J. Chem*., 2000, **24**(10), 739.
4 M. Y. Han and C. H. Quek, *Langmuir*, 2004, **20**, 3431.
5 F. R. F. Fan and A. J. Bard, *Science*, 1997, **277**, 1791.
6 M. Brust, J. M. Walker, D. Bethell, D. J. Schiffrin and R. Whyman, *J. Chem. Soc., Chem. Commun*., 1994, 801.
7 Y. Nakao, *J. Chem. Soc., Chem. Commun*., 1994, 2067.
8 K. S. Mayya and F. Caruso, *Langmuir*, 2003, **19**, 6987.
9 D. L. Feldheim and C. A. Foss, *Metal Nanoparticles. Synthesis Characterization and Application*, Marcel Dekker, Inc., New York, 2002.
10 S. Nath, S. K. Ghosh and T. Pal, *Chem. Commun*., 2004, 966.
11 K. George Thomas and P. V. Kamat, *J. Am. Chem. Soc*., 2000, **122**, 2655.
12 Y. Dirix, C. Bastiaansen, W. Caseri and P. Smith, *Adv. Mater*., 1999, **11**, 223.
13 J. B. Pendry, *Science*, 1999, **285**, 2590.
14 J. R. Krenn, A. Dereux, J. C. Weeber, E. Bourillot, Y. Lacroute and J. P. Coadennet, *Phys. Rev. Lett*., 1999, **82**, 2590.
15 E. J. Sanchez, L. Novotny and X. S. Xie, *Phys. Rev. Lett*., 1999, **82**, 4014.
16 B. Knoll and F. Kellmann, *Nature*, 1999, **399**, 134.
17 M. R. Pufall, A. Berger and S. Z. Schultz, *J. Appl. Phys*., 1997, **81**, 5689.
18 S. A. Maier, M. L. Brongersma, P. G. Kik, S. Meltzer, A. A. G. Requicha and H. A. Atwater, *Adv. Mater*., 2001, **13**, 1501.
19 S. A. Maier, P. G. Kik, H. A. Atwater, S. Meltzer, E. Harel, B. E. Koel and A. A. G. Requicha, *Nat. Mater*., 2003, **2**, 229.
20 P. C. Andersen and K. L. Rowlen, *Appl. Spectrosc*., 2002, **56**, 124.
21 G. Bauer, F. Pittner and T. Schalkhammer, *Mikrochim. Acta*, 1999, **131**, 107.
22 S. Löfås and B. Johnsson, *J. Chem. Soc., Chem. Commun*., 1990, **21**, 1526.
23 J. J. Storhoff, R. Elghanian, R. C. Mucic, C. A. Mirkin and R. L. Letsinger, *J. Am. Chem. Soc*., 1998, **120**, 1959.
24 R. Elghanian, J. J. Storhoff, R. C. Mucic, R. L. Letsinger and C. A. Mirkin, *Science*, 1997, **277**, 1078.
25 R. P. Van Duyne, J. C. Hulteen and D. A. Treichel, *J. Chem. Phys*., 1993, **99**, 2101.
26 M. D. Malinsky, K. L. Kelly, G. C. Schatz and R. P. Van Duyne, *J. Phys. Chem. B*, 2001, **105**, 2343.
27 U. Kreibig and M. Volmer, *Optical Propertiesof Metal Clusters*, Springer, Berlin, 1995.
28 C. L. Haynes and R. P. Van Duyne, *J. Phys. Chem. B*, 2001, **105**, 5599.
29 M. A. El-Sayed, *Acc. Chem. Res*., 2001, **34**, 257.
30 S. Link and M. A. El-Sayed, *J. Phys. Chem. B*, 1999, **103**, 8410.
31 U. Kreibig, M. Gartz, A. Hilger and H. Hovel, *Optical Investigations of Surfaces and Interfaces of Metal Clusters*, J. A. I. Press, Stamford, 1998, pp. 345–393.
32 P. Mulvaney, *Langmuir*, 1996, **12**, 788.
33 U. Kreibig, *Optics of Nanosized Metals*, CRC Press, Boca Raton, 1997, pp. 145–190.
34 J. C. Hulteen, D. A. Treichel, M. T. Smith, M. L. Duval, T. R. Jensen and R. P. Van Duyne, *J. Phys. Chem. B*, 1999, **103**, 3854.
35 L. M. Liz-Marzán and P. Mulvaney, *New J. Chem*., 1998, **22**(11), 1285.
36 G. Mie, *Ann. Phys. (Berlin)*, 1908, **25**, 377.
37 K. George Thomas, J. Zajicek and P. V. Kamat, *Langmuir*, 2002, **18**, 3722.
38 A. Manna, T. Imae, M. Iida and N. Hisamatsu, *Langmuir*, 2001, **17**, 6000.
39 K. K. Caswell, C. M. Bender and C. J. Murphy, *Nano Lett*., 2003, **3**, 667.
40 R. He, X. Qian, J. Yin and Z. Zhu, *J. Mater. Chem*., 2002, **12**, 3783.
41 N. R. Jana, T. K. Sau and T. Pal, *J. Phys. Chem. B*, 1999, **103**, 115.
42 T. Pal, T. K. Sau and N. R. Jana, *Langmuir*, 1997, **13**, 1481.
43 S. De, A. Pal, N. R. Jana and T. Pal, *J. Photochem. Photobiol., A*, 2000, **131**, 111.
44 A. Pal and T. Pal, *J. Raman Spectrosc*., 1999, **30**, 199.
45 S. Kundu, M. Mandal, S. K. Ghosh and T. Pal, *J. Colloid Interface Sci*., 2004, **272**, 134.
46 I. Pastoriza-Santos and L. M. Liz-Marzan, *Langmuir*, 1999, **15**, 948.
47 L. Zeiri and S. Efrima, *J. Phys. Chem*., 1992, **96**, 5908.
48 U. Kreibig and U. Genzel, *Surf. Sci*., 1985, **156**, 678.
49 N. J. Persson, *Surf. Sci*., 1993, **281**, 153.
50 O. Tzhayik, P. Sawant, S. Efrima, E. Kovalev and J. T. Klug, *Langmuir*, 2002, **18**, 3364.
51 A. Tanaka, Y. Takade, T. Nagasawa, H. Sasaki, Y. Kuriyama, S. Suzuki and S. Sato, *Surf. Sci*., 2003, **532–535**, 281–286.
52 F. Bensebaa, T. H. Ellis, E. Kruus, R. Voicu and Y. Zhou, *Langmuir*, 1998, **14**, 6579.
53 Z. Shen, Z. Zhao, H. Peng and M. Nygren, *Nature*, 2002, **417**, 266.
54 J. W. Mullin, *Crystallization*, Butterworth Heinemann, Woburn, MA, 3rd edn, 1997, pp. 172–202.
55 T. K. Sau and C. J. Murphy, *Langmuir*, 2005, **21**, 2928.
56 S. K. Ghosh, S. Nath, S. Kundu, K. Esumi and T. Pal, *J. Phys. Chem. B*, 2004, **108**, 13963.
57 A. J. Haes and R. P. Van Duyne, *Anal. Bioanal. Chem*., 2004, **379**, 920.
58 U. Kreibig and M. Vollmer, *Cluster materials*, Springer Berlin, Heidelberg, 1995, p. 532.
59 S. Underwood and P. Mulvaney, *Langmuir*, 1994, **10**, 3427.
60 P. V. Kamat, *J. Phys. Chem. B*, 2002, **106**, 7729.
61 *Active Metals: Preparation, Characterization, Applications*, ed. A. Fürstner, John Wiley & Sons, New York, 1995.
62 A. Henglein, P. Mulvaney and T. Linnert, *Faraday Discuss*., 1991, **92**, 31.

63 T. Ung, M. Giersig, D. Dunstan and P. Mulvaney, *Langmuir*, 1997, **13**, 1773.
64 A. C. Templeton, W. P. Wuelfing and R. W. Murray, *Acc. Chem. Res.*, 2000, **33**, 27.
65 M. P. Pileni, *J. Phys. Chem. B*, 2001, **105**, 3358.
66 A. Henglein, *J. Phys. Chem.*, 1993, **97**, 5457.
67 K. L. Kelly, E. Coronado, L. L. Zhao and G. C. Schatz, *J. Phys. Chem. B*, 2003, **107**, 668.
68 T. Linnert, P. Mulvaney and A. Henglein, *J. Phys. Chem.*, 1993, **97**, 679.
69 K. Boschkova, B. Kronberg, J. J. R. Stalgren, K. Persson and M. Ratoi Salagean, *Langmuir*, 2002, **18**, 1680.
70 A. C. Templeton, J. J. Pietron, R. W. Murray and P. Mulvaney, *J. Phys. Chem. B*, 2000, **104**, 564.
71 S. Nath, S. K. Ghosh, S. Kundu, S. Praharaj, S. Panigrahi and T. Pal, *J. Nanopart. Res.*, in press.
72 *Joint Committee on Powder Diffraction Standards* by JCPDS - International Centre for Diffraction Data, Newtown Square, PA, USA, 1997–2004.